# Systematic Analysis Method of E- and H-plane Circular Bend of Rectangular Waveguide based on the Planar Circuit Equations and Equivalent Network Representation

**Hsu,Jui-Pang and Tetsuo Anada**

**Faculty of Engineering ,Kanagawa University Yokohama, Japan 221**

## 1. Introduction

E- and H-plane circular bends of the rectangular waveguide, shown in Table 1(A), are very familiar waveguide components. So far, many works [1-4] have been done for the analysis of this structure, but their results are practically limited for the gradual bend case only. Therefore, wide-band frequency characteristics with wide range of bend parameters (=bend angle and curvature*) including sharp bend are still not clear, but are needed for the future microwave integrated circuit design. This paper solves these problems by the following procedure.

1. Derivation of terminal mode impedance which leads to the equivalent network representation, based on the planar circuit theory and normal mode analysis.
2. Calculation of the equivalent network parameters. Especially, calculation of radial mode function is the key step; non-uniform transmission line analogy and numerical analysis is utilized in our case.
3. Wide-band frequency characteristics (V.S.W.R) of E- and H-plane right angle circular bend are calculated for wide range of bend curvature by our method.

Through these analysis, E- and H-plane circular bend can be treated in the same way because they are ruled by the same planar circuit equations.

(*bend curvature parameter : $C=b/a$, $0<C<1$)

## 2. Derivation of equivalent network representation – multi-transmission lines circuit –

E- or H-plane curved rectangular waveguide shown in Table 1(A) can be considered to be a E- or H-plane planar circuit as a whole. Therefore, as demonstrated by (B)-(E) in Table 1, the 3-D field distribution in these structure including input/output waveguide can be fully described by the following planar circuit equations.

$$\begin{cases} \mathrm{grad}V = -jXJ \\ \mathrm{div}J = -jBV \end{cases} \qquad (1)$$

where series reactance X and shunt susceptance B with the boundary condition are given by (G), (F) in Table 1 for E- and H-plane planar circuit, respectively.

In order to solve these planar circuit equations systematically under the given boundary conditions, the curved waveguide is divided into the straight and circular bend section, where x-y coordinate system is replaced by l-s rectangular or r-θ cylindrical coordinate system, respectively. Then, as explained in Table 2 and 3, the equivalent multi-transmission lines circuit in each section is derived based on the separation of variables technique and modal analysis.

**Table 1 E-plane and H-plane planar circuit equations and boundary condition for E- and H-plane circular bend.**

| | | | |
|---|---|---|---|
| **Circular bend and Curvature parameter** | 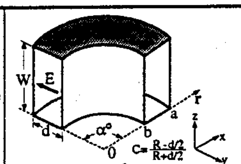 (a) E-Plane α° Bend | 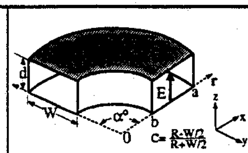 (b) H-Plane α° Bend | A |
| **3-D Field** | $\mathbf{E}=(\mathbf{E}_t,0)$ , $\mathbf{H}=(\mathbf{H}_t,\mathbf{H}_z)$ | $\mathbf{E}=(\mathbf{E}_t,\mathbf{E}_z)$ , $\mathbf{H}=(\mathbf{H}_t,0)$ | B |
| **Field component** $k_0=\omega\sqrt{\varepsilon_0\mu_0}$ | $E_t(x,y,z)=E_t(x,y)\cdot\sqrt{2}\sin\frac{\pi z}{W}$ <br> $H_z(x,y,z)=H_z(x,y)\cdot\sqrt{2}\sin\frac{\pi z}{W}$ <br> $H_t(x,y,z)=H_t(x,y)\cdot\frac{\sqrt{2}\pi}{k_0 W}\cos\frac{\pi z}{W}$ | $H_t(x,y,z)=H_t(x,y)$ <br> $E_z(x,y,z)=E_z(x,y)$ <br> $E_t(x,y,z)=0$ | C |
| **Voltage Current** | $V^H=-H_z(x,y)\cdot d$ (A) <br> $J^H=\mathbf{k}\times E_t(x,y)$ (V/m) | $V^E=-E_z(x,y)\cdot d$ (V) <br> $J^E=H_t(x,y)\times\mathbf{k}$ (A/m) | D |
| **Planar Circuit Equations with B. C.** | $\begin{cases}\mathrm{grad}V^H=-jX^HJ^H \\ \mathrm{div}J^H=-jB^HV^H\end{cases}$ | $\begin{cases}\mathrm{grad}V^E=-jX^EJ^E \\ \mathrm{div}J^E=-jB^EV^E\end{cases}$ | E |
| | $\frac{\partial V^H}{\partial n}=0$ (or $J^H\cdot n=0$) | $V^E=0$ (or $J^E\times n=0$) | F |
| **Planar Immittance** | $X^H=\frac{\beta_t^2 W}{\omega\mu_0}$ , $B^H=\frac{\omega\mu_0}{W}$ | $X^E=\frac{\beta_t^2 d}{\omega\varepsilon_0}$ , $B^E=\frac{\omega\varepsilon_0}{d}$ | G |
| **propagation constant** | $\beta_t^H=\sqrt{k_0^2-(\pi/W)^2}$ | $\beta_t^E=k_0=\omega\sqrt{\varepsilon_0\mu_0}$ | H |





CH3577-4/95/0000-0749$01.00 © 1995 IEEE

Mode characteristic impedance, mode propagation constant and mode function in each section are given or defined in table 2, 3 and 4(A).

Here, the whole equivalent network is shown in Fig. 1, where the coupling between propagation modes in the straight and circular bend section at the junction is represented by ideal transformer, whose transformer ratio between n-th mode in the circular bend and p-th mode in the i-th input/output waveguide is given by eq.(2).

$$n_{np}^{(i)} = \frac{1}{(a-b)}\int_b^a R_n(r) f_p(s^{(i)})dr \qquad (2)$$

In Fig. 1, $Z_{cn}$ and $Z'_{cn}$, $\nu_n$ and $\beta_n$ are characteristic impedance and propagation constant at circular and straight section given by (C) in Table 2 and Table 3, respectively. Then terminal mode impedance between i-th port p-th mode (i,p) and j-th port q-th mode (j,q) are given by the following equation.

$$\mathbf{Z_{pq}} = \sum_n \begin{pmatrix} n_{np}^{(1)} & 0 \\ 0 & n_{np}^{(2)} \end{pmatrix} \cdot \begin{pmatrix} -jZ_{cn}\cot\nu_n\alpha & -jZ_{cn}\csc\nu_n\alpha \\ -jZ_{cn}\csc\nu_n\alpha & -jZ_{cn}\cot\nu_n\alpha \end{pmatrix} \begin{pmatrix} n_{nq}^{(1)} & 0 \\ 0 & n_{nq}^{(2)} \end{pmatrix} \qquad (3)$$

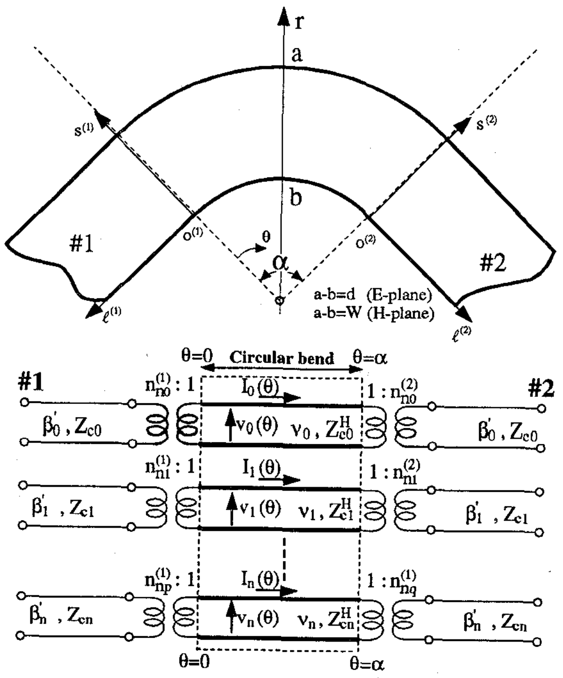


**Fig.1 Coordinate system and equivalent multi-transmission lines circuit.**

**Table 2 Equivalent transmission line model of straight waveguide section.**

| E-plane | H-plane | |
|---|---|---|
| Coordinate system (l,s) | Coordinate system (l,s) | |
| 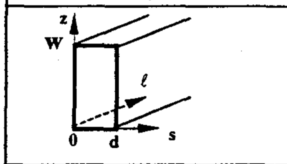 | 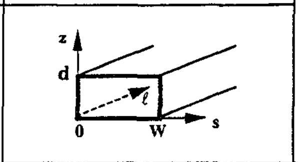 | A |
| **Separation of variable with p-th mode width function $f_p(s)$** | | |
| $V_p^H(\ell,s)=V_p^H(\ell)f_p^H(s)$<br>$J_{\ell p}^H(\ell,s)=[I_p^H(\ell)/d]f_p^H(s)$<br>$J_{sp}^H(\ell,s)=j\frac{1}{X^H}V_p^H(\ell)f_p^{H'}(s)$<br>$f_p^H(s)=\sqrt{\varepsilon_n}\cos(p\pi s/d)$<br>$p=0,1,2,\cdots$ | $V_p^E(\ell,s)=V_p^E(\ell)f_p^E(s)$<br>$J_{\ell p}^E(\ell,s)=[I_p^E(\ell)/W]f_p^E(s)$<br>$J_{sp}^E(\ell,s)=j\frac{1}{X^E}V_p^E(\ell)f_p^{E'}(s)$<br>$f_p^E(s)=\sqrt{2}\sin(p\pi s/W)$<br>$p=1,2,\cdots$ | B |
| **Transmission line equations along *l* for p-th width mode** | | |
| 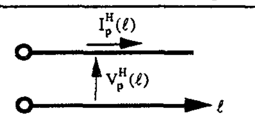<br>$\frac{dV_p^H}{d\ell}=-jX_p^H I_p^H,\ X_p^H=\frac{X^H}{d}$<br>$\frac{dI_p^H}{d\ell}=-jB_p^H V_p^H,\ B_p^H=\frac{(\beta_p^H)^2}{X^H}d$<br>$Z_{cp}^{'H}=\frac{X^H}{\beta_p^H d}$<br>$\beta_p^H=\sqrt{(\beta_t^H)^2-(p\pi/d)^2}$ | 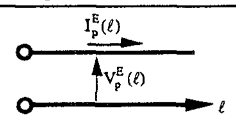<br>$\frac{dV_p^E}{d\ell}=-jX_p^E I_p^E,\ X_p^E=\frac{X^E}{d}$<br>$\frac{dI_p^E}{d\ell}=-jB_p^E V_p^E,\ B_p^E=\frac{(\beta_p^E)^2}{X^E}W$<br>$Z_{cp}^{'E}=\frac{X^E}{\beta_p^E W}$<br>$\beta_p^E=\sqrt{(\beta_t^E)^2-(p\pi/W)^2}$ | C |

**Table 3 Equivalent transmission line model for circular bend section.**

| E-plane (r,θ) | H-plane (r,θ) | |
|---|---|---|
| 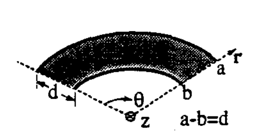<br>(a) E-plane circular bend | 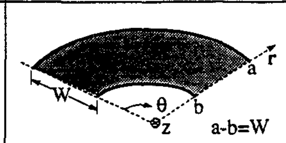<br>(b) H-plane circular bend | A |
| **Separation of variable for voltage and current with radial function $R_n(r)$** | | |
| $V_n^H(r,\theta)=V_n^H(\theta)\cdot R_n^H(r)$<br>$J_{\theta n}^H(r,\theta)=I_n^H(\theta)\cdot R_n^H(r)/r$<br>$J_{rn}^H(r,\theta)=j\frac{1}{X^H}V_n^H(\theta)\cdot R_n^{H'}(r)$<br>$R_n^H(r)$ : see table 4 $(n=0,1,2,\cdots)$ | $V_n^E(r,\theta)=V_n^E(\theta)\cdot R_n^E(r)$<br>$J_{\theta n}^E(r,\theta)=I_n^E(\theta)\cdot R_n^E(r)/r$<br>$J_{rn}^E(r,\theta)=j\frac{1}{X^E}V_n^E(\theta)\cdot R_n^{E'}(r)/r$<br>$R_n^H(r)$ : see table 4 $(n=0,1,2,\cdots)$ | B |
| **Transmission line equations along θ for n-th radial mode** | | |
| 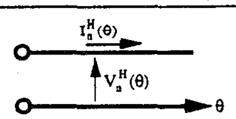<br>$\frac{dV_n^H}{d\theta}=-jX^H I_n^H$<br>$\frac{dI_n^H}{d\theta}=-j\frac{(\nu_n^H)^2}{X^H}V_n^H$<br>$\nu_n^H$ : circular propagation constant<br>$Z_{cn}^H=\frac{X^H}{\nu_n^H}$ | 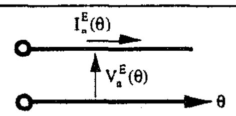<br>$\frac{dV_n^E}{d\theta}=-jX^E I_n^E$<br>$\frac{dI_n^E}{d\theta}=-j\frac{(\nu_n^E)^2}{X^E}V_n^E$<br>$\nu_n^E$ : circular propagation constant<br>$Z_{cn}^E=\frac{X^E}{\nu_n^E}$ | C |

## 3. Calculation of radial mode function with the help of non-uniform transmission line analogy

As explained by (A) in Table 4, radial mode function $R_n(r)$ and circular propagation constant $\nu_n$ are the solution of the following eigenvalue equation, whose boundary condition(B.C.) is given in Table 4.

$$\frac{1}{r}\frac{d}{dr}\left(r\frac{dR_n}{dr}\right)+\left(\beta_t^2-\frac{\nu_n^2}{r^2}\right)\cdot R_n=0 \qquad (4)$$

When $\beta_t=0$, analytical solution is obtained and given by (B) in Table 4 for E and H-plane circular bend, respectively. However analytical solution is impossible for $\beta_t \neq 0$. Therefore, how to solve the eigenvalue equation (4) for $\beta_t \neq 0$ is the key process in our analysis. As shown by (C) in Table 4, replacing R(r) by v(r) and defining i(r) as jr dR/dr, second order differential equation (4) can be transformed to a pair of first order differential equations.

$$\frac{dv}{dr}=-jx(r)i \ , \quad \frac{di}{dr}=-jb(r)v \qquad (5)$$

where $x(r)=1/r$ , $b(r)=\beta_t^2 r-\nu^2/r$

These equations can be understood as a voltage-current relation along the non-uniform transmission line as shown in Fig.2.

In order to find $R_n$ and $\nu_n$ numerically for a given $\beta_t$, this non-uniform transmission line between b and a is equally divided into N small sections, so as to make each section be approximated by uniform transmission line. Then, assuming $\nu$, total F-matrix between b and a can be calculated numerically by F-matrix product of N sections, resulting eq.(6)

$$\begin{pmatrix} v_b \\ i_b \end{pmatrix}=\begin{pmatrix} A_t & B_t \\ C_t & D_t \end{pmatrix}\begin{pmatrix} v_a \\ i_a \end{pmatrix} \qquad (6)$$

Numerical search of $\nu_n$, which makes $C_t=0$, gives $\nu_n^H$ and then $R_n^H(r)$. Also $B_t=0$ gives $\nu_n^E$ and $R_n^E(r)$. Thus calculated example of E-plane circular bend are shown in Fig.3 (d/W=0.5); $\nu_n^H$ as a function of normalized frequency F for C=0.01 and corresponding normal mode function $R_n^H(r)$ at F=1.0 and F=1.5 up to 5-th mode.

When $\beta_t=0$(F=1.0), $R_n(r)$ and $\nu_n$ are analytically obtained by (B) in Table 4 . No difference between the numerical results (F=1.0) and analytical results(F=1.0) in Fig.3 proves the validity of the above numerical computation. In our calculation N is taken as 200, which is enough for sufficient calculation accuracy.

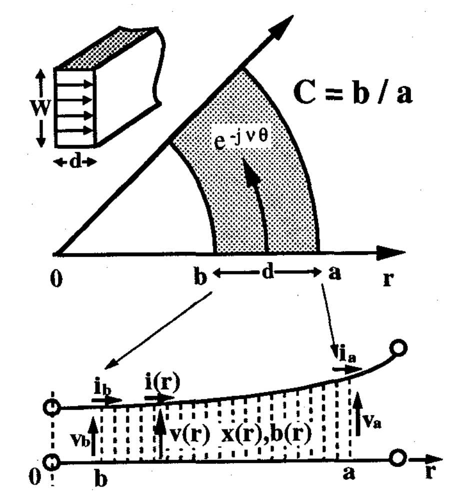


**Fig.2 Non-uniform transmission line model and its step-like approximation.**

## 4. Frequency characteristics of V.S.W.R of right angle circular bend

Based on equivalent network shown in Fig. 1, V.S.W.R of E-and H-plane right angle circular bend with wide range

**Table 4 Radial normal mode function in circular bend.**

| E-plane | H-plane | |
|---|---|---|
| $R_n$ : n-th radial normal mode | $\nu_n$ : n-th circular propagation constant | A |
| $\frac{1}{r}\frac{d}{dr}(r\frac{dR_n^H}{dr})+[(\beta_t^H)^2-\frac{(\nu_t^H)^2}{r^2}]R_n^H=0$ <br> $(\beta_t^H)^2=k_0^2-(\pi/W)^2$ <br> B.C. $\frac{dR_n^H}{dr}=0$ $(r=a,b)$ <br> $\int_b^a\frac{R_m^H(r)R_n^H(r)}{r}dr=\delta_{mn}$ | $\frac{1}{r}\frac{d}{dr}(r\frac{dR_n^E}{dr})+[(\beta_t^E)^2-\frac{(\nu_t^E)^2}{r^2}]R_n^E=0$ <br> $(\beta_t^E)^2=k_0^2$ <br> B.C. $R_n^E=0$ $(r=a,b)$ <br> $\int_b^a\frac{R_m^E(r)R_n^E(r)}{r}dr=\delta_{mn}$ | |
| Anatical solution for βt=0 | | B |
| $R_n^H(r)=\sqrt{\frac{\varepsilon_n}{\ln C}}\cos\left[\frac{n\pi}{\ln C}\ln\frac{r}{a}\right]$ <br> $\nu_n^H=-j\frac{\pi}{\ln C}n$ $(n=0,1,2,\cdots)$ <br> C=b/a | $R_n^E(r)=\sqrt{\frac{2}{\ln C}}\sin\left[\frac{n\pi}{\ln C}\ln\frac{r}{a}\right]$ <br> $\nu_n^E=-j\frac{\pi}{\ln C}n$ $(n=1,2,\cdots)$ <br> C=b/a | |
| Numerical solution for βt≠0 by non-uniform transmission line | | C |
| $v(r)=R_n^H(r)$ , $i(r)=jr\cdot\frac{dR_n^H}{dr}$ <br> $\begin{cases}\frac{dv}{dr}=-jx(r)i(r)\\ \frac{di}{dr}=-jb(r)v(r)\end{cases}$ <br> $x=1/r$ , $b=(\beta_t^H)^2r-\nu^2/r$ <br> B.C. $i(r)=0$ $(r=a,b)$ | $v(r)=R_n^E(r)$ , $i(r)=jr\cdot\frac{dR_n^E}{dr}$ <br> $\begin{cases}\frac{dv}{dr}=-jx(r)i(r)\\ \frac{di}{dr}=-jb(r)v(r)\end{cases}$ <br> $x=1/r$ , $b=(\beta_t^E)^2r-\nu^2/r$ <br> B.C. $v(r)=0$ $(r=a,b)$ | |

of bend curvature is calculated for the frequency band where only dominant mode propagates. Hence, the higher modes in the input/output waveguide are terminated by the corresponding reactive mode impedance. The results are shown in Fig.4. In these analysis, enough number of higher modes (evanescent modes) in each region are taken into consideration( for example, 14 evanescent modes for C=0.01 case).

## 5. Conclusion

Systematic analysis method to calculate the frequency characteristics of E- and H-plane circular bend of any bend angle and curvature for the rectangular waveguide is proposed and wide band frequency characteristics of 90°bend angle are calculated for wide range of bend curvature including sharp bend by this method.

## Literature


1. S.O.Rice, "Reflection from circular bends in rec angular waveguides-matrix theory,", Bell Syst. Tech. J.., vol.27
2. J.A. Cochran and R.G. Pecina, "Mode propagation in continuously curved waveguides,", Radio Science, vol.1, no.6
3. L. Lewin, "Theory of Waveguides,", New York Wiley, 1975
4. V.K.Tripathi,etc, "A rigorous and efficient method of moments solution for curved waveguide bends,", IEEE MTT vol.40, no.12, Dec. 1992.


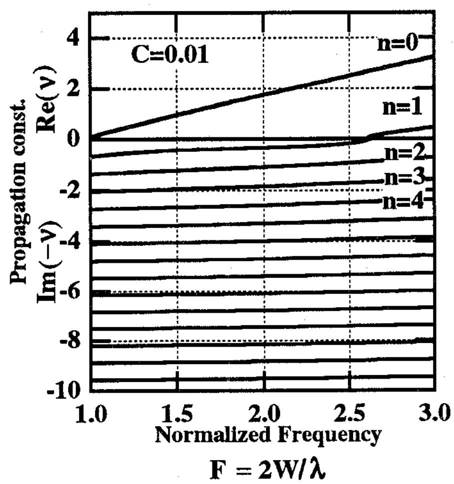


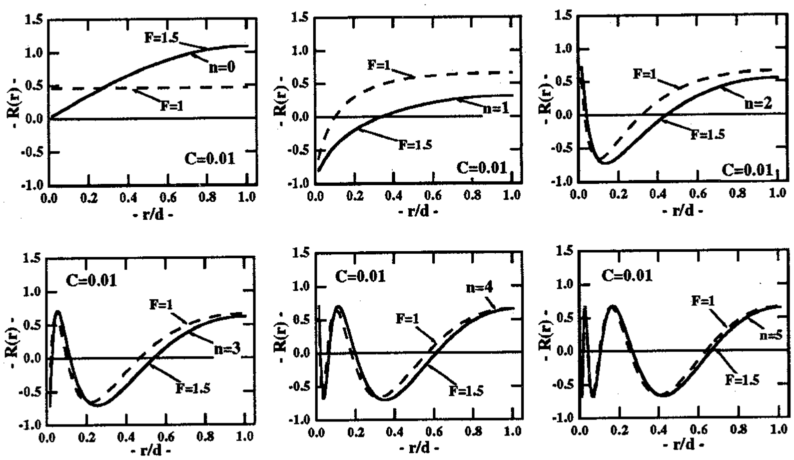


Fig.3 Circular propagation constant ν and radial normal mode function R(r) (F=1.0 and F=1.5) for E-plane circular bend(d=W/2). Broken line also includes analytical results of Table 4(B).

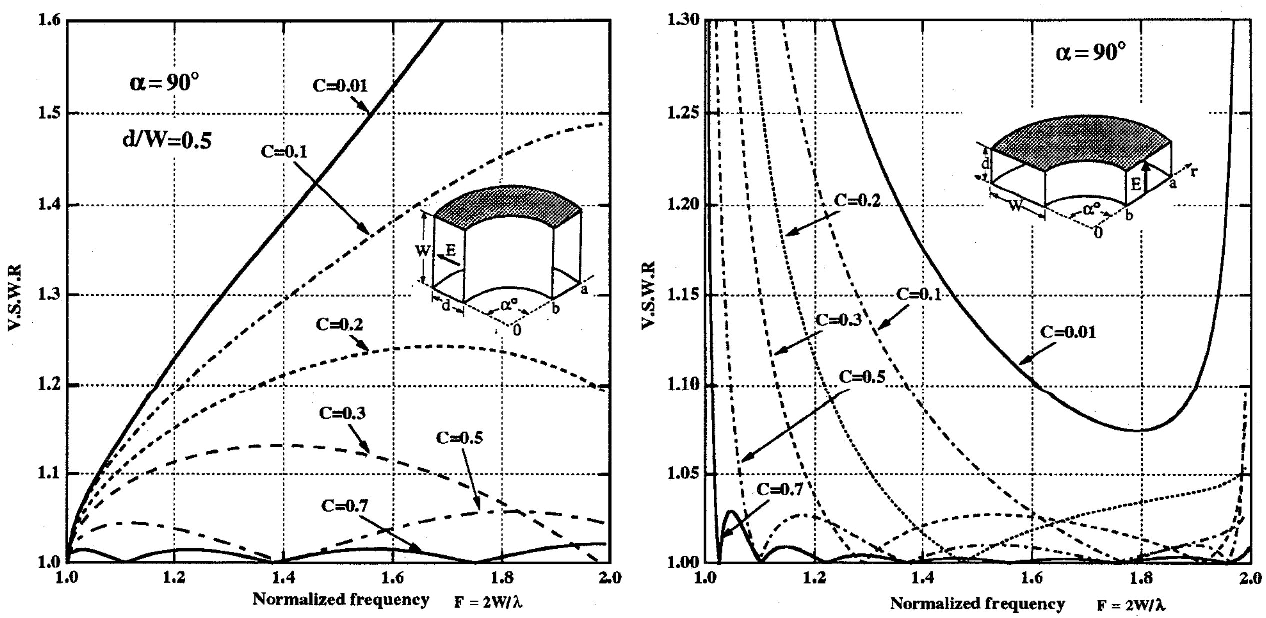


(a) E-plane right angle circular bend

(b) H-plane right angle circular bend

**Fig.4 Frequency characteristics(V.S.W.R) of E- and H-plane right angle circular bend.**